



UNITED NATIONS EDUCATIONAL, SCIENTIFIC AND CULTURAL ORGANIZATION
INTERNATIONAL ATOMIC ENERGY AGENCY
INTERNATIONAL CENTRE FOR THEORETICAL PHYSICS
I.C.T.P., P.O. BOX 586, 34100 TRIESTE, ITALY, CABLE: CENTRATOM TRIESTE



H4.SMR/1013-21

**SCHOOL ON THE USE OF SYNCHROTRON RADIATION
IN SCIENCE AND TECHNOLOGY:
*"John Fuggle Memorial"***

3 November - 5 December 1997

Miramare - Trieste, Italy

X-ray monochromators

**F. Boscherini
INFN - Laboratori Nazionali Frascati
Frascati, Italy**

X-RAY MONOCHROMATORS

F. Boscherini

INFN - Lab. Naz. Frascati

- Dynamical Diffraction Theory (Results)
- Basic Monochromator Designs
- X-Ray Optics of Sagittal Focussing with x-tals
- Dispersive XAFS Optics
- Very High Resolution Instruments

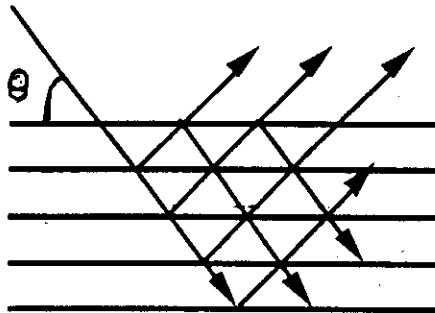
DYNAMICAL DIFFRACTION THEORY: INTRODUCTION

- The more commonly used theory for diffraction is the kinematical theory. Scattering from each atom is considered once:

$$F(\vec{q}) = \sum_{i=1}^{\infty} f_i \exp(i\vec{q} \cdot \vec{r}_i)$$

Normally a good approximation because charge scattering of x-rays is weak.

- Dynamical theory considers the multiple interactions of the x-ray wave field within the crystal.



$$\lambda = 2d \sin \theta$$

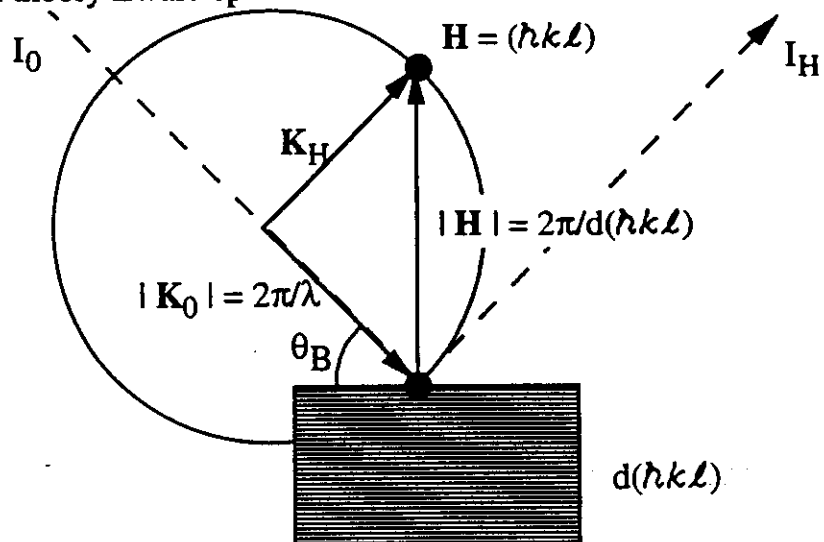
It is necessary when large, perfect crystals are involved (e.g. Si, Ge...).

Remember: $\lambda \approx$ interatomic distance.

- Dynamical effects can be observed also with small crystals.
Primary extinction: decrease in intensity of strong peaks.
- We will treat dynamical theory in view of the following applications:
 - ⇒ Standing waves method.
 - ⇒ X-ray Optics.

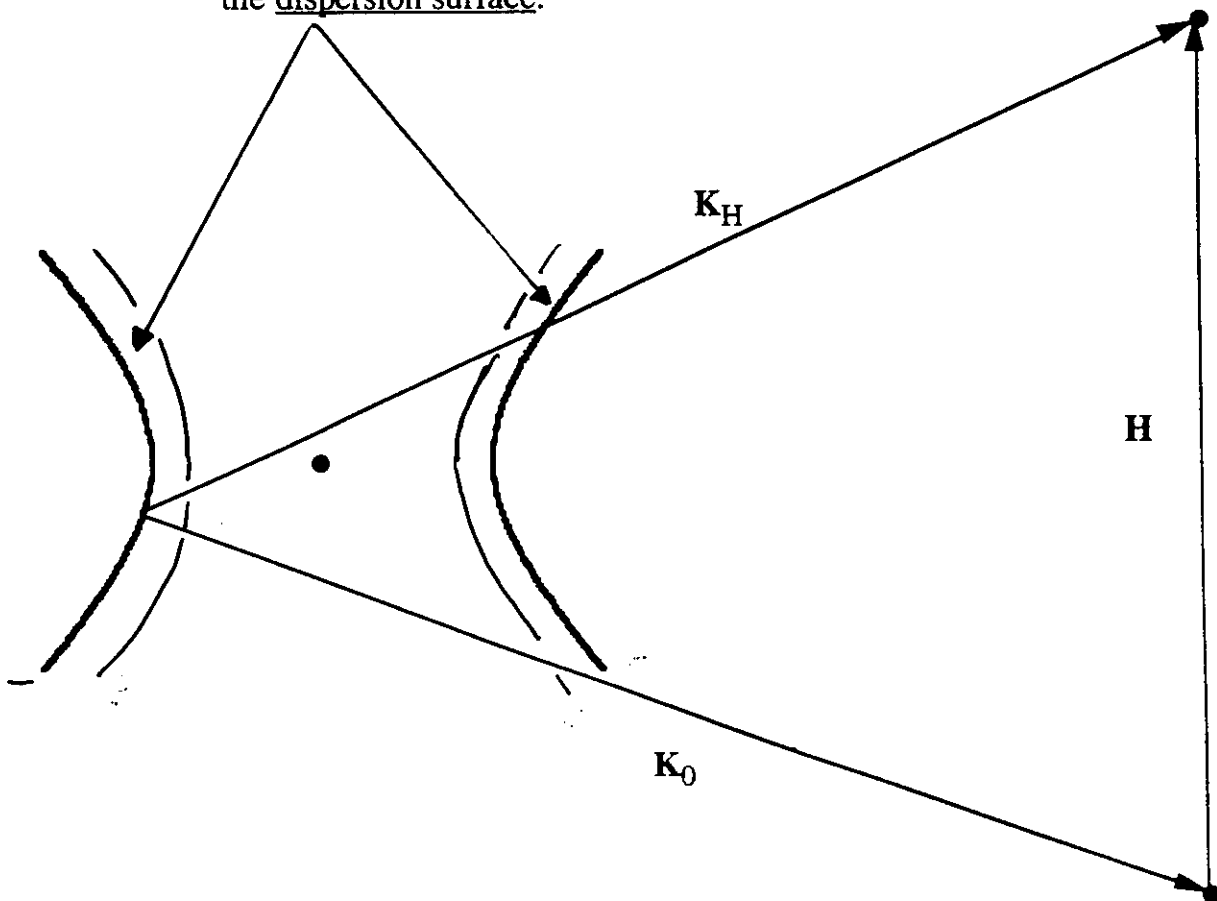
DYNAMICAL DIFFRACTION THEORY: MODIFICATION OF EWALD SPHERE CONSTRUCTION

- Kinematical theory Ewald sphere construction:



- In dynamical theory:

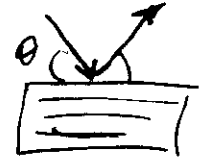
⇒ no longer a single Ewald sphere for each monochromatic ray;
 ⇒ there exists a continuum of centers of allowed Ewald spheres,
 the dispersion surface.



DYNAMICAL DIFFRACTION THEORY: THE SYMMETRIC BRAGG CASE 1

- The field amplitude is given by (centrosymmetric crystal):

$$\frac{E_H}{E_0} = \eta \pm \sqrt{(\eta^2 - 1)} = \sqrt{R} \exp(i\phi)$$



where

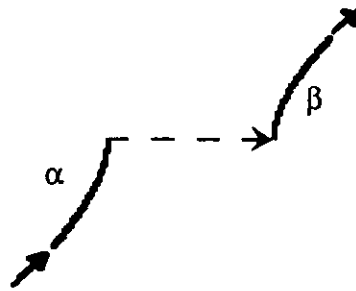
$$\eta = \frac{-\Delta\theta \sin 2\theta_B + \Gamma F_H}{\Gamma F_H} \text{ is the angular deviation parameter.}$$

$$\Delta\theta = \theta - \theta_B$$

$$\lambda = 2d \sin \theta_B$$

$$F_H = \sum_i f_i \exp(i\mathbf{H} \cdot \mathbf{r}_i)$$

$$\Gamma = \frac{r_e \lambda^2}{\pi V}$$



- For $-1 < \eta < 1$, E_H/E_0 is imaginary \Rightarrow there is total external reflection.

This is the Darwin width: $\omega_D = 2\Gamma F_H / \sin 2\theta_B$

At 8 keV:	Si(111)	36 μ rad
	Si(311)	15 μ rad

The Darwin width determines the intrinsic resolution of a monochromator crystal:

$$\frac{\Delta\lambda}{\lambda} = \omega_D \cot \theta_B$$

$$\lambda = 2d \sin \theta$$

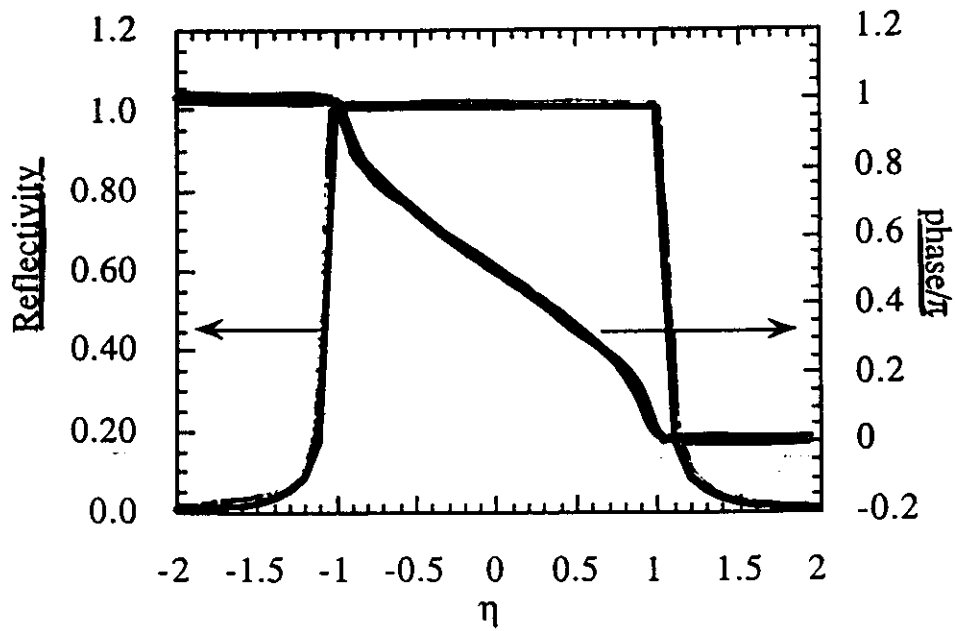
- The penetration depth in the region of total reflection is the:

$$\text{extinction length} = 2 \sin \theta_B / (\pi^2 \Gamma F_H)$$

1 or 2 orders of magnitude smaller than normal photoelectric absorption.

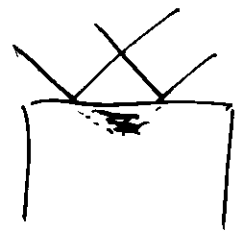
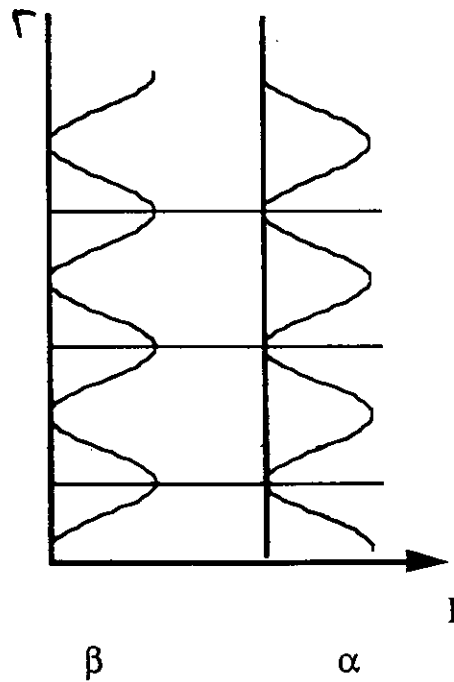
At 8 keV:	Si(111)	1 μ m	
	Si(311)	2.7 μ m	compare to 64 μ m

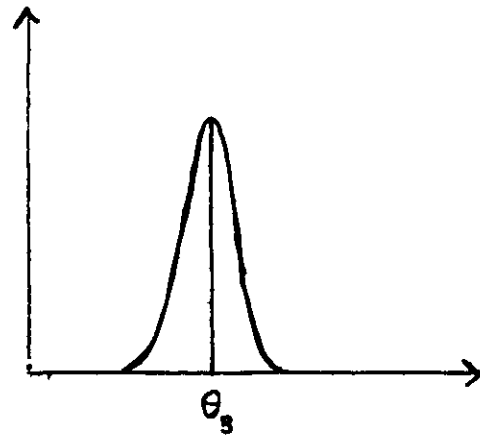
DYNAMICAL DIFFRACTION THEORY:
THE SYMMETRIC BRAGG CASE 2



- The phase change by π shows that relative phase of the two fields changes in the region of total external reflection.
- The two fields E_0 and E_H interfere to generate a standing wave field.

Its intensity is: $I = |E_H + E_0|^2 = 1 + R + 2\sqrt{R} \text{Cos} [\phi - 2\pi\mathbf{H}\cdot\mathbf{r}]$





Kinematical Theory

Broadening due to

- size
- mosaic spread
- defects

Darwin width is intrinsic to perfect crystal

X-ray monochromators

Table 2
Intrinsic Bragg reflection widths ω , energy resolutions $\Delta E/E$ and integral reflecting powers I of perfect crystals of silicon, germanium and α -quartz at 1.54 Å.

Crystal	hkl	ω (second of arc)	$\Delta E/E$ ($\times 10^3$)	I ($\times 10^3$)	
Silicon	111	7.395	14.1	39.9	
	220	5.459	6.04	29.7	
	311	3.192	2.90	16.5	
	400	3.603	2.53	19.3	
	331	2.336	1.44	11.8	
	422	2.925	1.47	15.5	
	333				
	(511)	1.989	0.88	9.9	
	440	2.675	0.96	14.0	
	531	1.907	0.69	9.3	
Germanium	111	16.338	32.64	85.9	
	220	12.449	14.46	67.4	
	311	7.230	6.92	37.1	
	400	7.951	5.94	42.3	
	331	5.076	3.34	25.4	
	422	6.178	3.34	32.4	
	333				
	(511)	4.127	2.00	20.2	
	440	5.339	2.14	27.5	
	531	3.719	1.33	17.7	
α -quartz	100	3.798	10.00	18.8	
	101	7.453	15.26	40.9	
	110	2.512	3.69	12.2	
	10 $\bar{2}$	2.488	3.36	12.9	
	200	2.252	2.81	11.5	
	112	2.927	3.03	15.5	
	202	2.072	1.93	10.6	
	212	2.042	1.47	10.7	
	20 $\bar{3}$	2.430	1.74	12.9	
	301	2.368	1.69	12.6	

$$\frac{\Delta E}{E} = \omega_s \cot \theta_s = \frac{\Gamma F_H}{\sin^2 \theta} \sim d_H^2 F_H$$

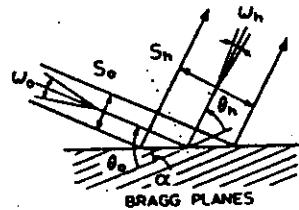
$$\lambda = 2d \sin \theta$$

$$\frac{\Delta \lambda}{\lambda} = \Delta \theta \cot \theta$$

DYNAMICAL DIFFRACTION THEORY: ASYMMETRIC BRAGG CASE

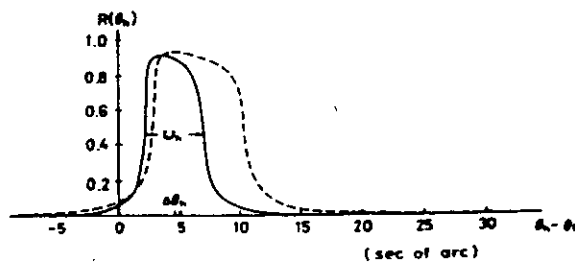
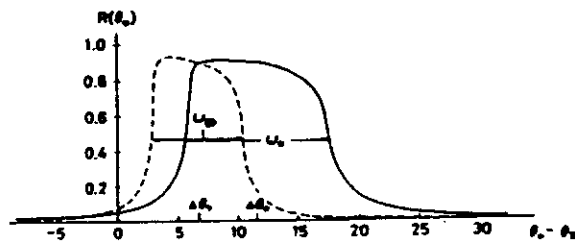
- The asymmetry factor is:

$$b = \frac{\sin(\theta_B - \alpha)}{\sin(\theta_B + \alpha)}$$



- The input and output reflection widths are modified:

$$\omega_0 = \frac{\omega_D}{\sqrt{b}} \qquad \omega_H = \omega_D \sqrt{b}$$



- The beam cross sections also change:

$$\omega_H S_H = \omega_0 S_0$$

DYNAMICAL DIFFRACTION THEORY:
EFFECT OF POLARIZATION AND HARMONICS

- For π polarization the Darwin width decreases by a factor $|\cos 2\theta_B|$

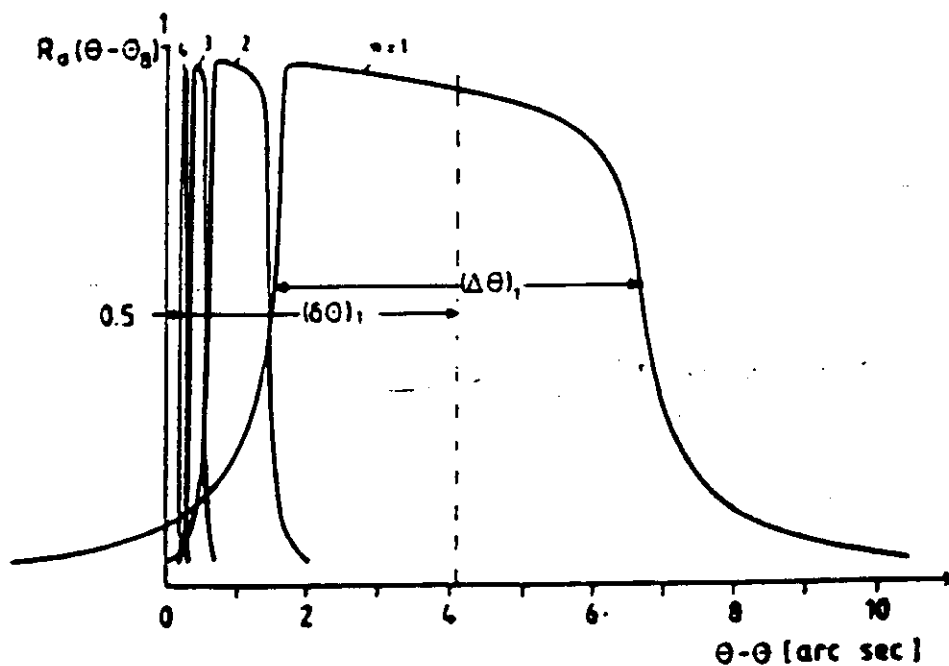
⇒ Use vertical dispersion for most common SR sources.

- For a given angular setting harmonics can be transmitted by the crystal:

$$\lambda = (1/n) 2d \sin \theta$$

The reflectivity curve for higher harmonics has:

- 1) smaller shift with respect to θ_B (shift $\propto 1/n^2$ at least)
- 2) smaller width (width $\propto 1/n^2$ at least)



PRINCIPLES OF MONOCHROMATOR DESIGN: FLAT CRYSTAL CONFIGURATIONS

- Consider a point source of X-rays with divergence Ω and a flat crystal with Darwin width ω_D .

The central reflected ray has a wavelength:

$$\lambda_0 = 2d \sin \theta_0$$

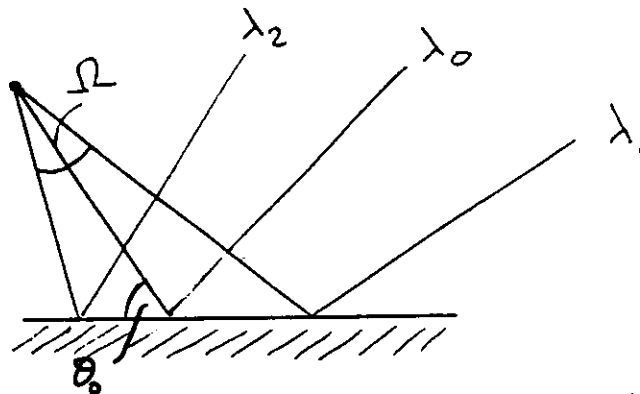
The minimum and maximum wavelengths reflected are:

$$\lambda_1 = 2d \sin (\theta_0 - \Omega/2 - \omega_D/2)$$

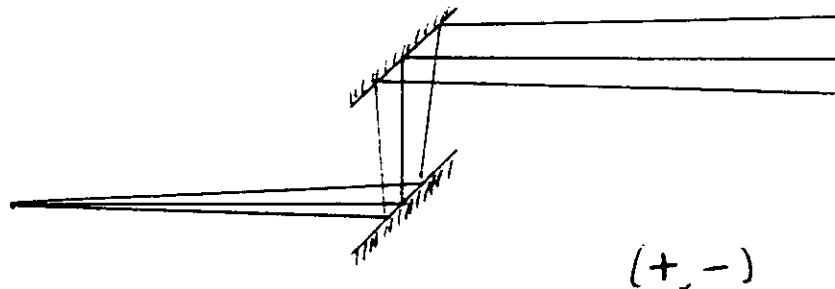
$$\lambda_2 = 2d \sin (\theta_0 + \Omega/2 + \omega_D/2)$$

and the band-pass is:

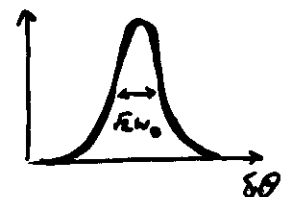
$$\Delta\lambda/\lambda = (\Omega + \omega_D) \cot \theta_0$$



- For two parallel crystals (+,-) every ray transmitted by the first crystal will also be transmitted by the second (band-pass equal to single crystal case).

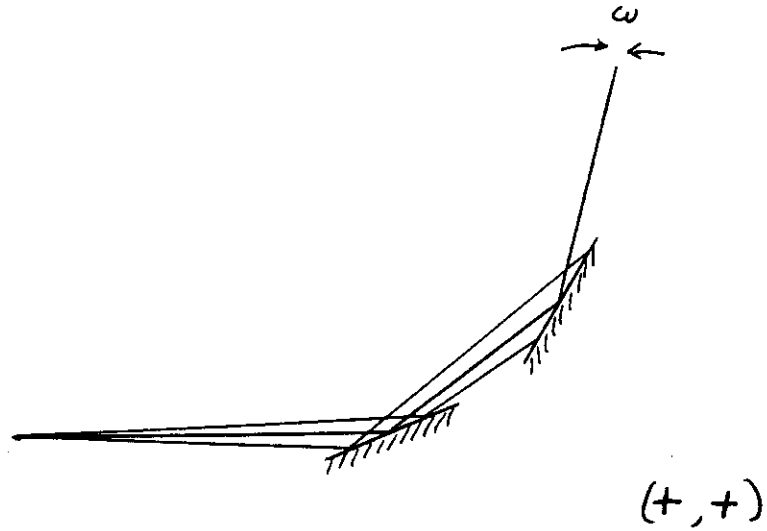


A scan of the relative alignment of the two crystals yields the double crystal rocking curve, independent of beam divergence.

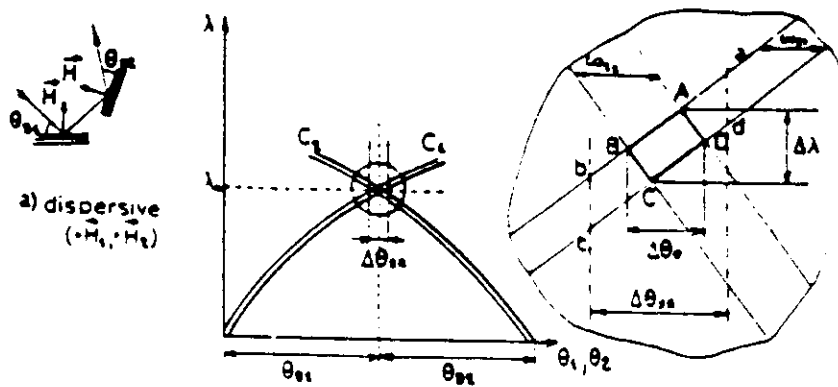
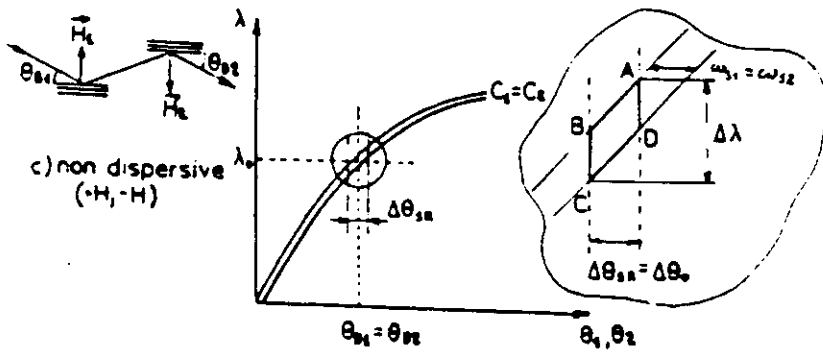
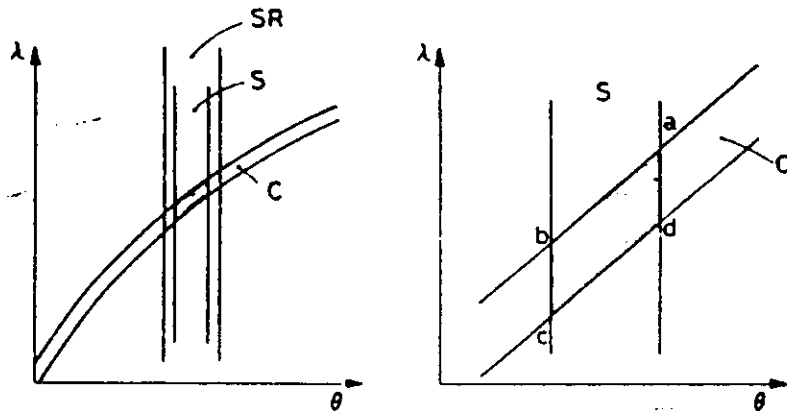


PRINCIPLES OF MONOCHROMATOR DESIGN:
FLAT CRYSTAL CONFIGURATIONS

- For the anti-parallel configuration (+,+) only those rays with equal divergence within ω_D will be transmitted (high resolution configuration).



DIAGRAMMI DI DUMOND

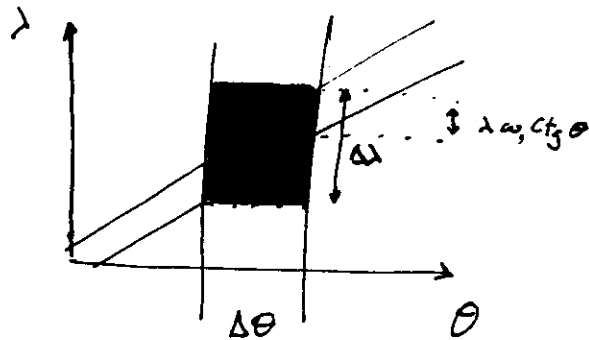


$$\overline{F}_I = \frac{F \left(\frac{\Delta \lambda}{\lambda} = 10^{-3} \right)}{10^{-3}} \times \frac{\Delta \lambda}{\lambda} \times \frac{\omega_0}{\omega_0 + \Delta \omega} \times \frac{\Delta \theta}{3\sigma_R}$$

$$\overline{F}_I = \frac{F \left(\frac{\Delta \lambda}{\lambda} = 10^{-3} \right)}{10^{-3}} \omega_0 \cot^2 \theta \frac{\Delta \theta}{3\sigma_R}$$

$$\overline{I} = \frac{F_I}{F \left(\frac{\Delta \lambda}{\lambda} = 10^{-3} \right)} = \frac{\omega_0 \cot^2 \theta}{10^{-3}} \frac{\Delta \theta}{3\sigma_R}$$

————— || —————



$$\text{Incidente} = \Delta \lambda \cdot \Delta \theta = \lambda \cot^2 \theta [\omega + \Delta \omega] \cdot \Delta \theta$$

$$\text{Trasverso} = \lambda \omega_0 \cot^2 \theta \Delta \theta$$

$$\frac{T}{I} = \frac{\omega}{\omega + \Delta \omega}$$

DUMOND DIAGRAMS FOR ASYMMETRIC CRYSTALS

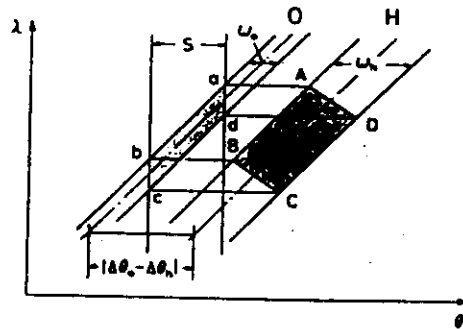


Fig. 6. DuMond diagram describing an asymmetric crystal after a slit of opening angle S . The system admits X-rays represented by $abcd$ and transmits them to $ABCD$. The figure is drawn for $b > 1.0$ (see text for further explanation).

Band pass depends on

- incident divergence (cd)
- width of acceptance curve (da)

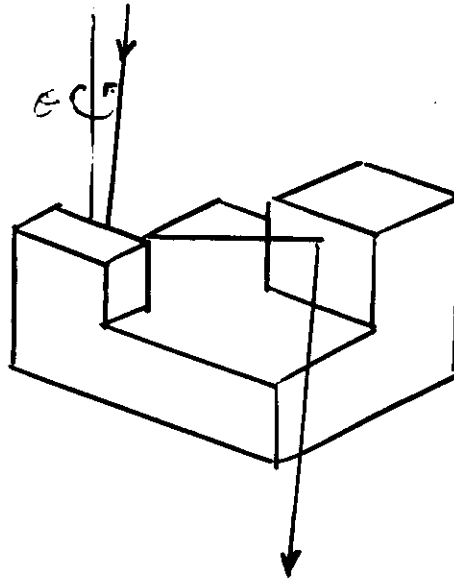
w_0/\sqrt{b}

CHANNEL CUT MONOCHROMATOR

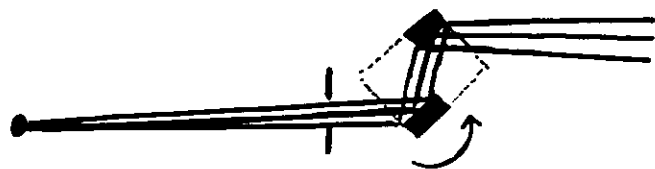
- Cut a groove inside a single crystal bloc to obtain (+,-) configuration.

Advantages: simplicity
 low cost

Disadvantages: no harmonics rejection
 beam height changes with angle ($\Delta z = 2 G \cos \theta$)



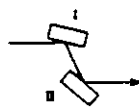
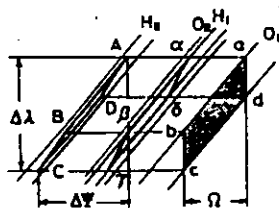
- The band-pass is given by:



$$\Delta\lambda/\lambda = (\Omega_{\text{source}} + \Omega_{\text{slits}} + \omega_{DI}/b^{1/2}) \cot \theta_0$$

$$\Omega_{\text{source}} = (\text{source size}) / (\text{source - mono distance})$$

$$\Omega_{\text{slits}} = (\text{slit setting}) / (\text{source - slit distance})$$



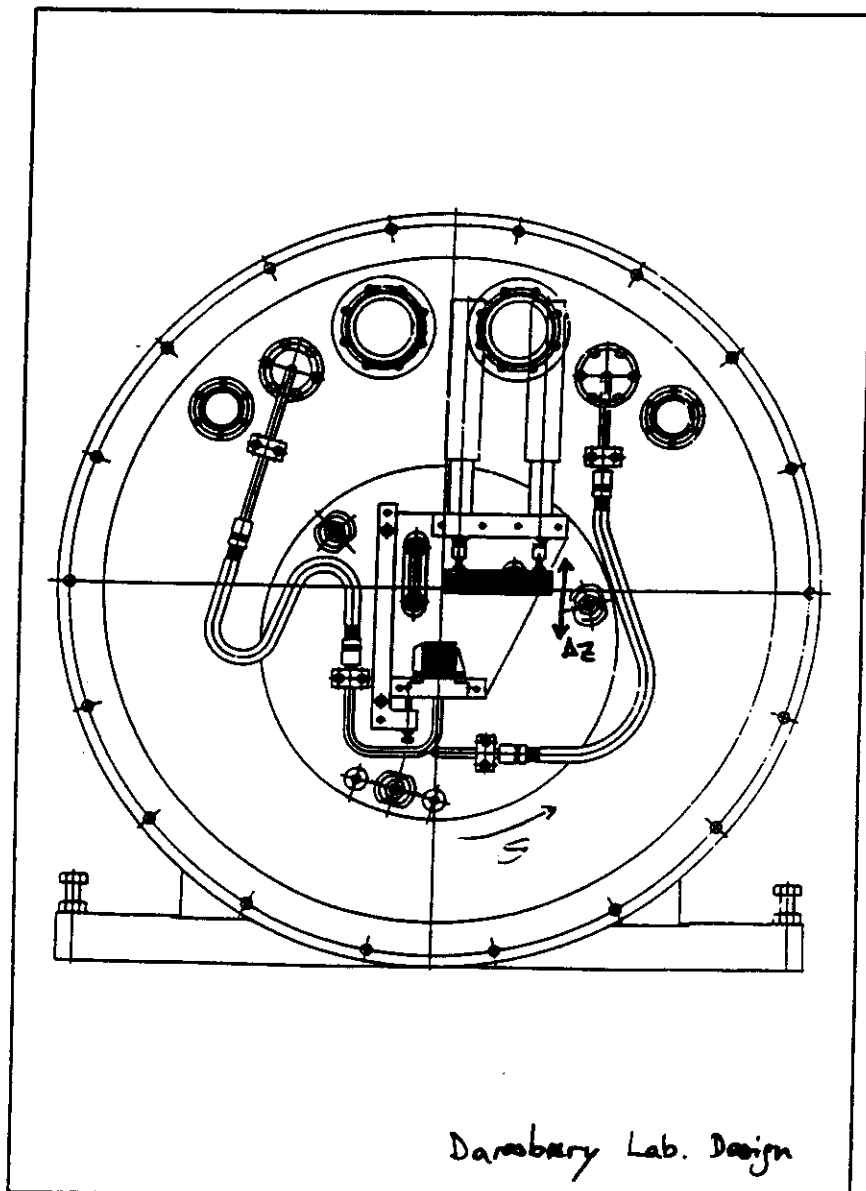
$+n - n$

DOUBLE CRYSTAL MONOCHROMATOR

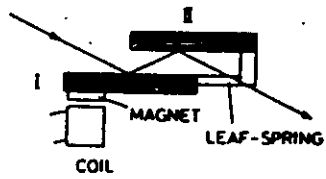
- The two crystals are now independent.

Advantages: harmonics rejection possible
beam height can be constant
more degrees of freedom

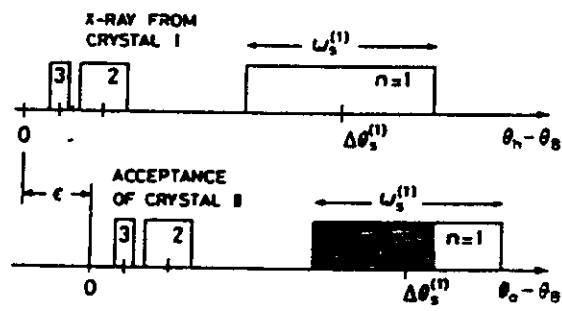
Disadvantages: cost



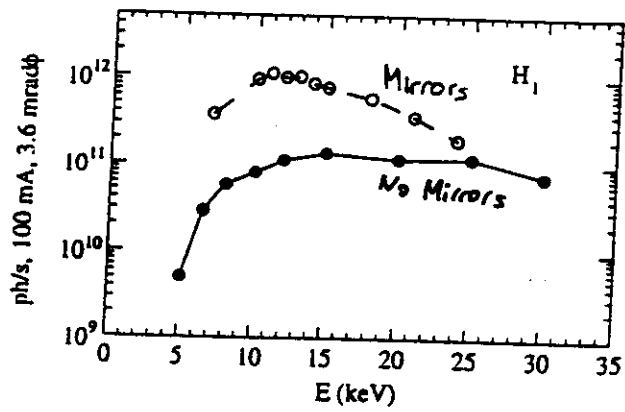
HARMONICS REJECTION BY CRYSTAL DETUNING



(a)

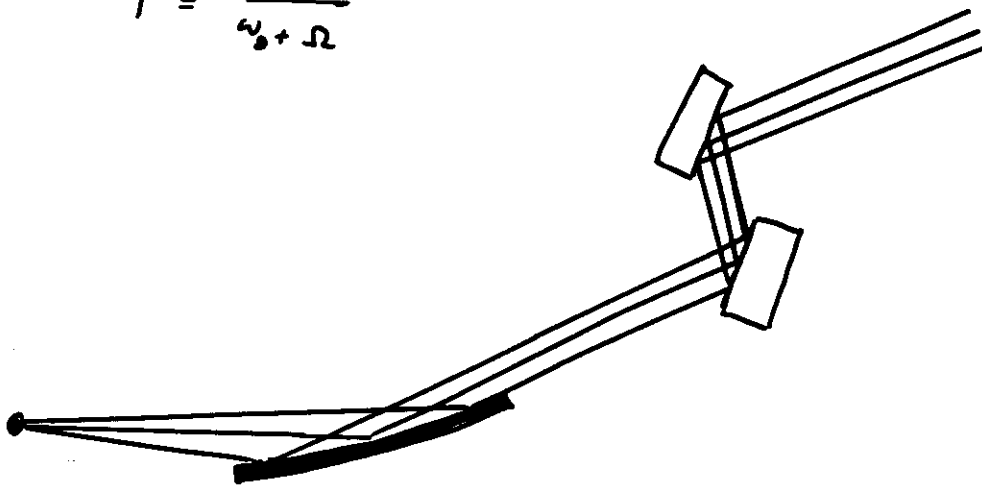


INCREASING MONOCHROMATOR TRANSMISSION USING A COLLIMATING MIRROR



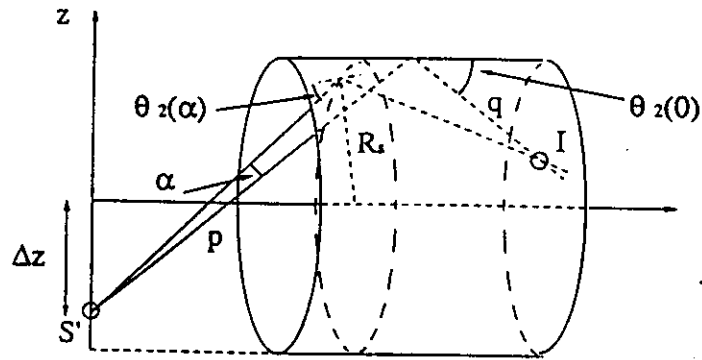
GILDA D/L
ESRF

$$T = \frac{\Omega_0}{\Omega_0 + \Omega}$$

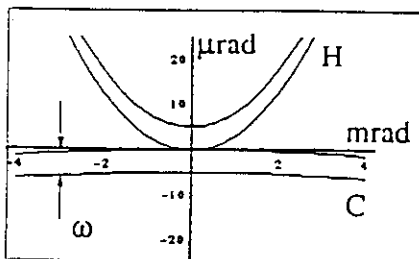
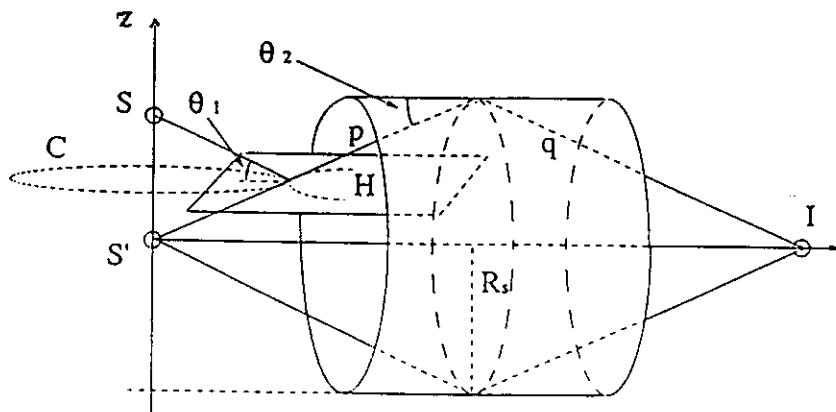


Sagittal focussing of x-rays with bent crystals: introduction

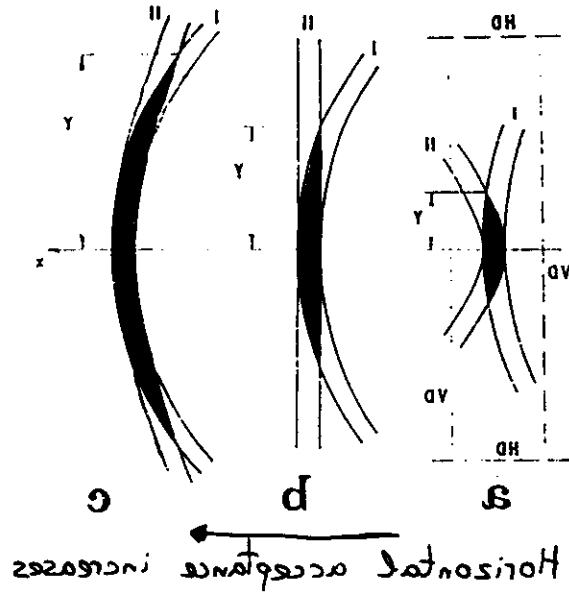
Pascarelli, Boscherini, D'Acapito, Hrdy, Meneghini and Mobilio, *J. Synch. Rad.* 3, 147 (1996)



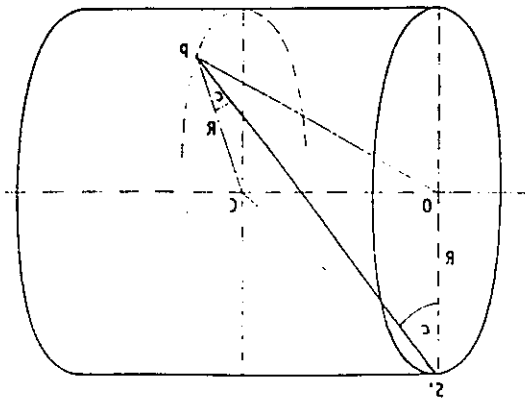
- Magnification is: $M = q/p = 1/[1 + (2 \frac{\Delta z}{R_s})]$
- Horizontal acceptance determined by: $\theta_2(\alpha) - \theta_2(0) = \omega_D$



Sagittal focusing of x-rays with bent crystals: introduction

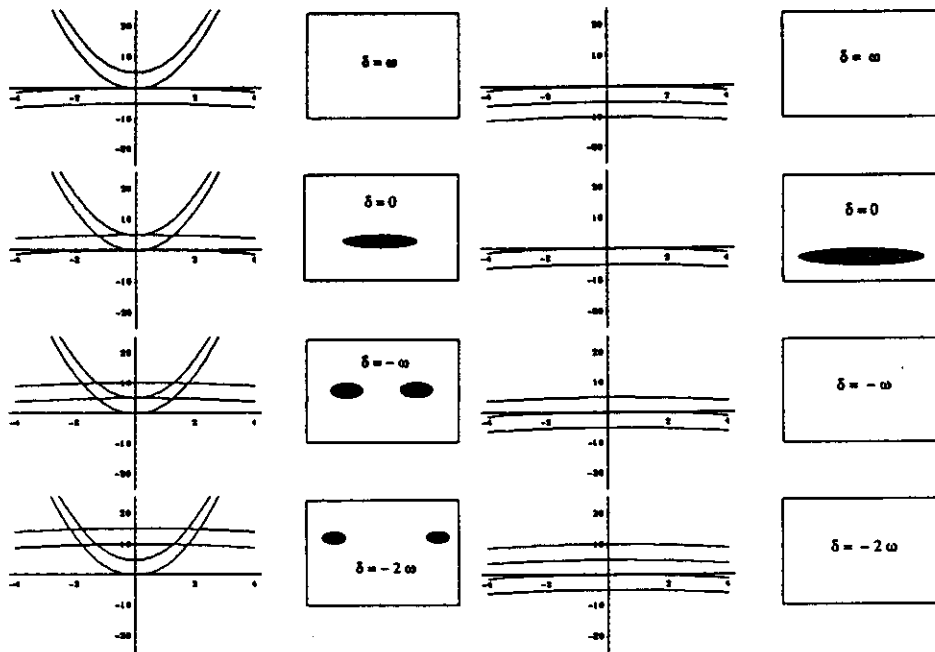


- a) $\Delta z = 0; M = 1$
 b) $\Delta z = R \cos \theta; M = |1 + 2 \cos \theta| = 1/3$ (Sparks, 1980).
 c) $R \cos \theta < \Delta z < R$;
 When $\Delta z = R, M = 1/3$ and there is total transmission (Hrdy, 1994).

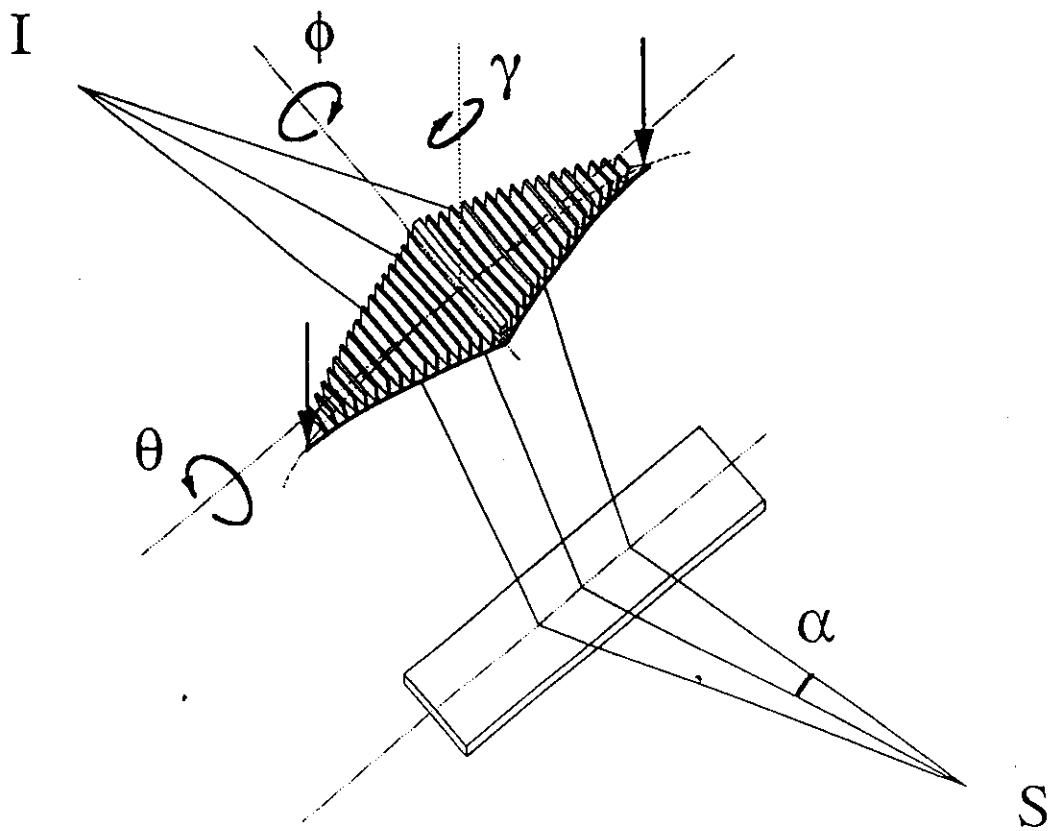


Sagittal focussing of x-rays with bent crystals: simulation of beam footprints

Si(311) 25 keV

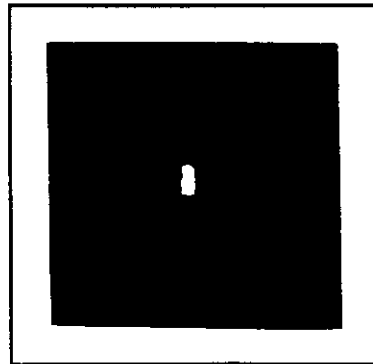


Sagittal focussing of x-rays with bent crystals: monochromator design



SAGITTAL FOCUSING

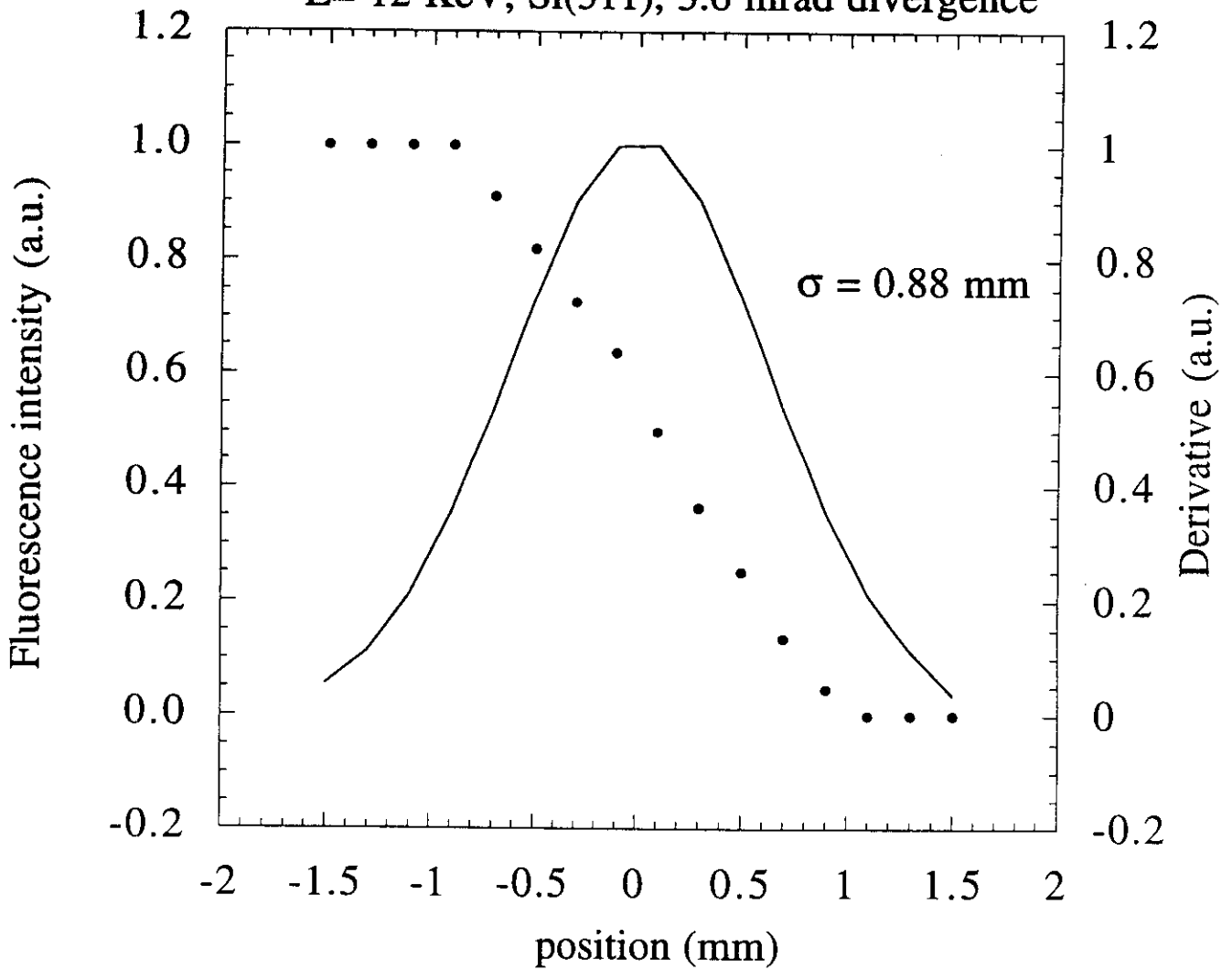
Crystal: Si(311)
Energy range: 6-25 keV
Average Photon Density Gain: 50



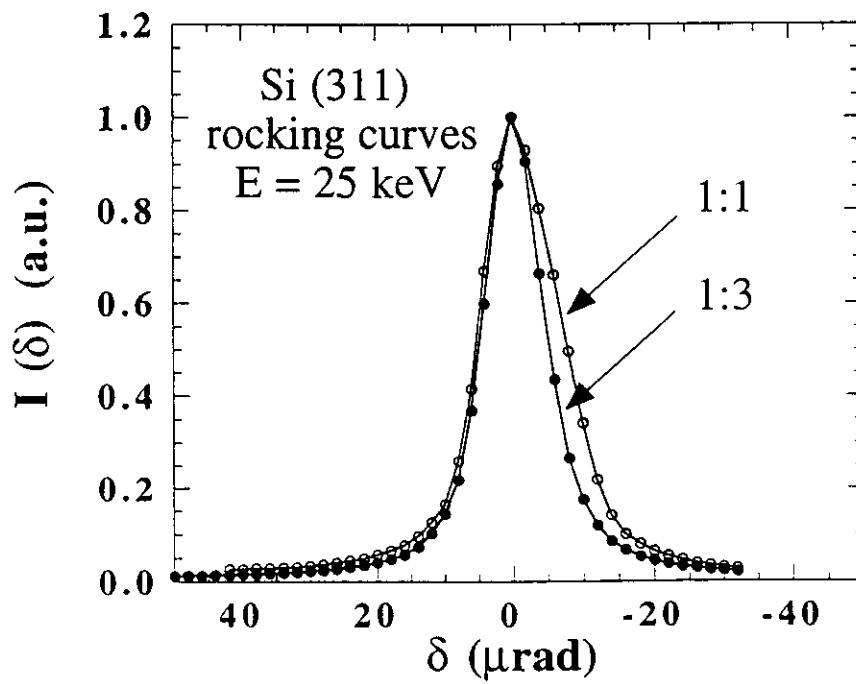
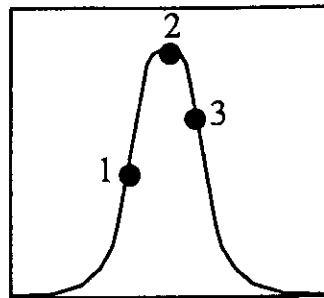
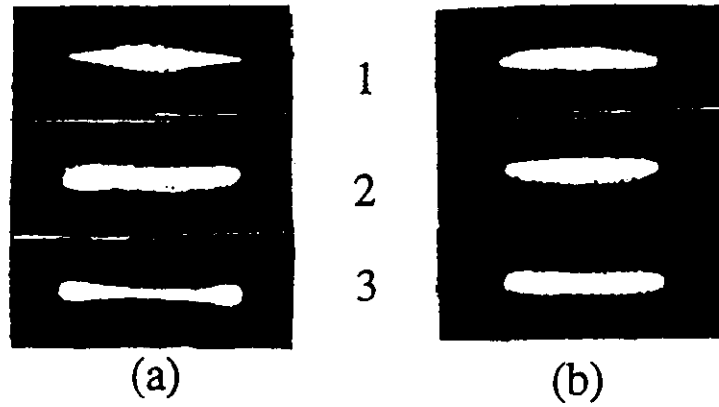
Example @ 15 keV

(beam not vertically focused)

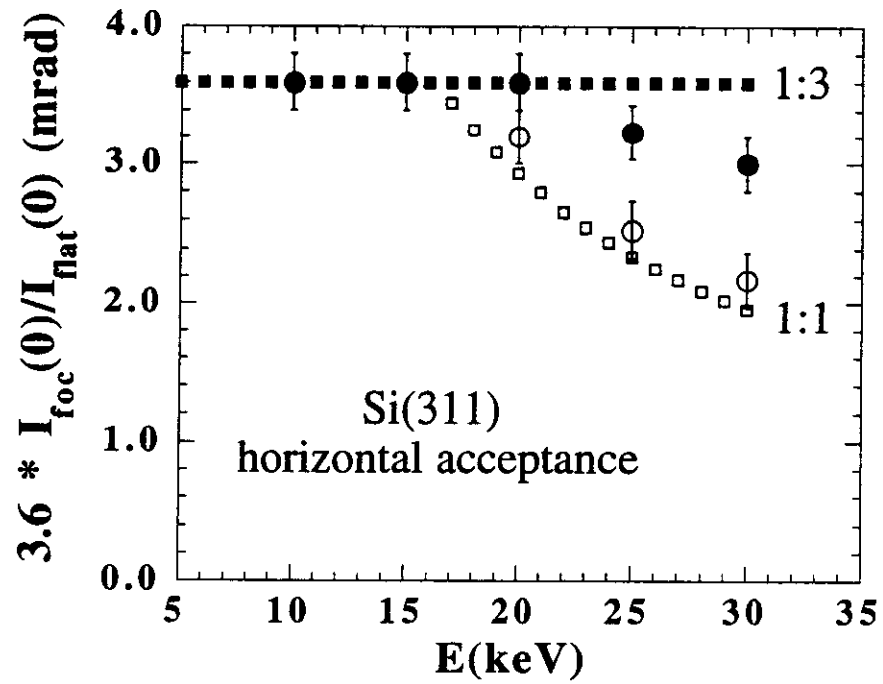
GILDA
Dynamical sagittal focussing
Horizontal beam profile
E= 12 KeV, Si(311), 3.6 mrad divergence



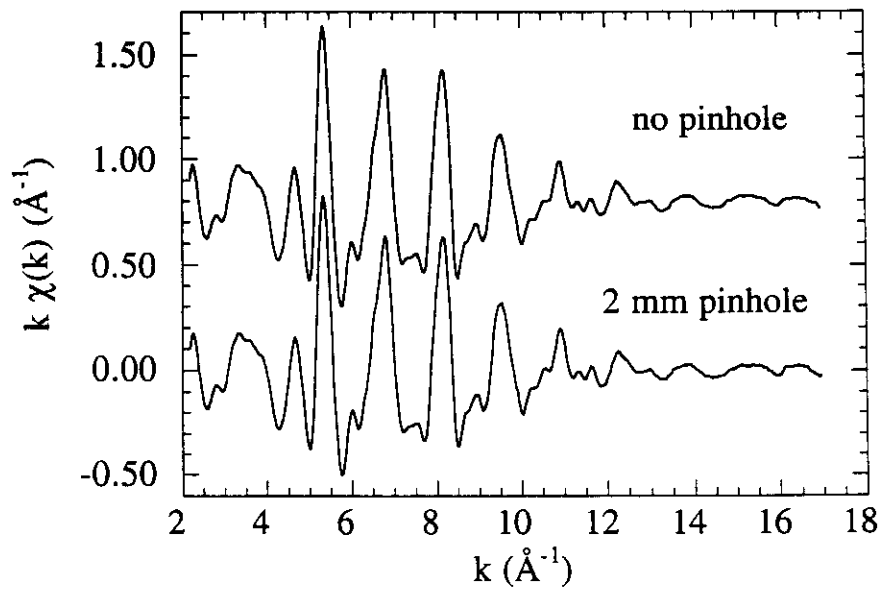
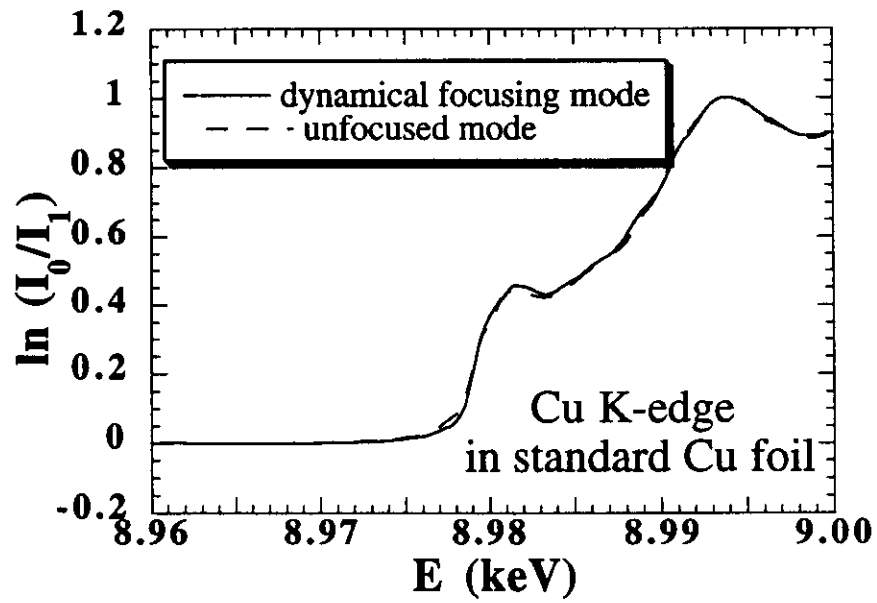
Sagittal focussing of x-rays with bent crystals: images of beam and rocking curves



Sagittal focussing of x-rays with bent crystals: horizontal acceptance

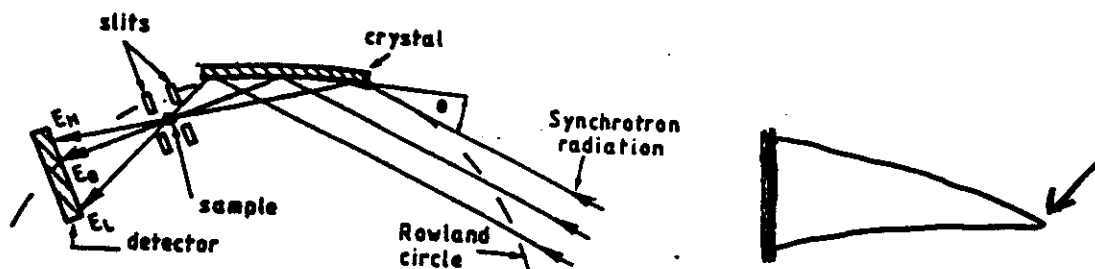


Sagittal focussing of x-rays with bent crystals: resolution and spot size



OPTICS OF DISPERSIVE X-RAY ABSORPTION SPECTROMETERS 1

- X-ray absorption spectroscopy in the dispersive geometry:
 - ⇒ Time resolved studies in the milli-second time scale (parallel acquisition)
 - ⇒ High-pressure (small spot)
 - ⇒ Dichroism (high stability, use of quarter-wave plates)



- For curved crystal optics (tangential focussing):

$$1/r + 1/r' = 2/(R \sin \Theta_0)$$

r = source - crystal distance

r' = crystal - focus distance

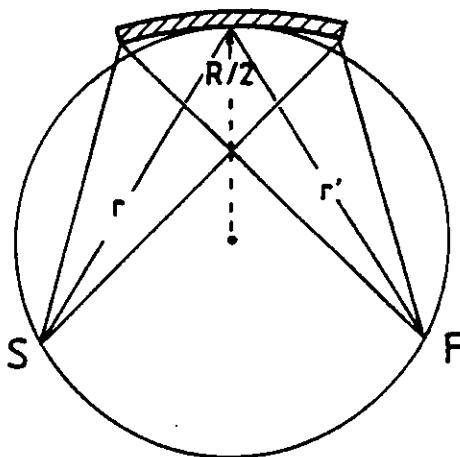
Θ_0 = Bragg angle

- The symmetrical solution is:

$$r=r' = R \sin \Theta_0$$

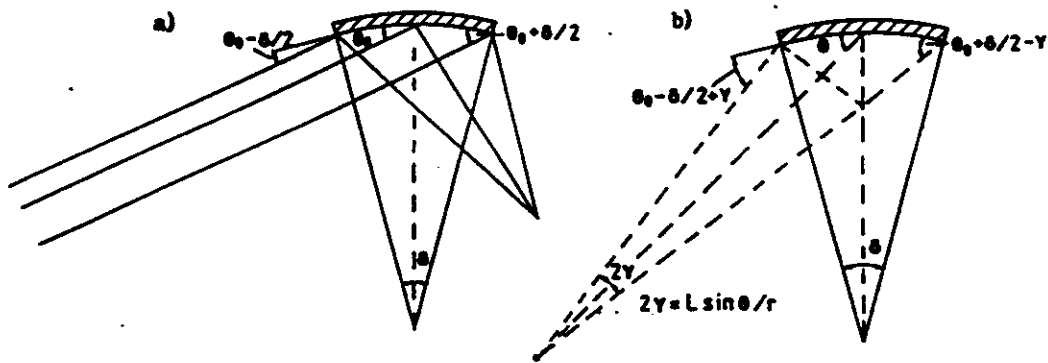
Rowland circle geometry:

The source and the monochromatic focus lie on the Rowland circle ($R/2$).



OPTICS OF DISPERSIVE X-RAY ABSORPTION SPECTROMETERS 2

- In the case of a SR source $r \equiv \infty$
 $r' \equiv R \sin \theta_0 / 2$ and we have a polychromatic focus.



- Energy dispersion

$$\Delta E/E = \Omega \cot \theta_0$$

$$\Omega \text{ (total divergence)} = \{(\text{collected divergence})^2 + (\text{source size})^2 + (\text{intrinsic})^2\}^{1/2}$$

$$\Omega_1 = (L/R - L \sin \theta_0 / r)$$

$$\Omega_2 = \Delta s / r$$

$$\Omega_3 = \omega_D$$

Typically $\Delta E = 400 - 1000 \text{ eV}$

OPTICS OF DISPERSIVE X-RAY ABSORPTION SPECTROMETERS 3

• Energy resolution

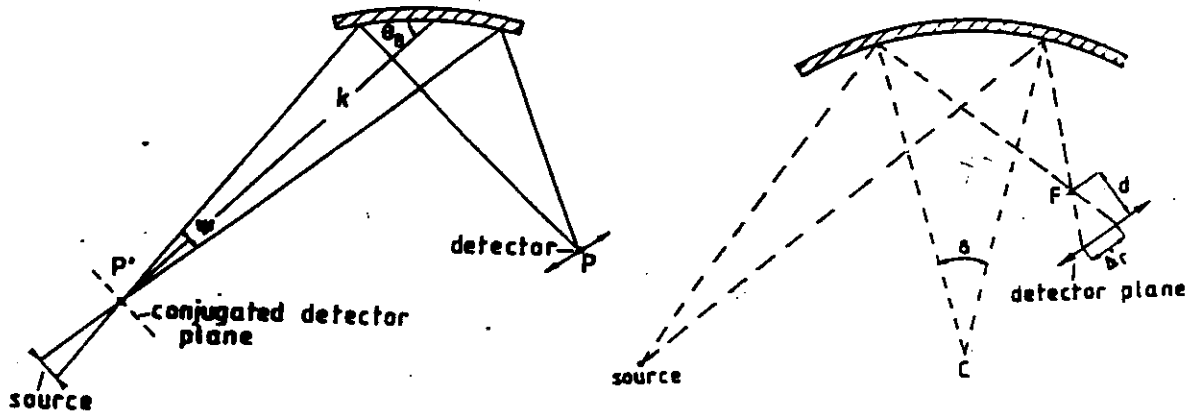
$$\delta E/E = \omega \cot \theta_0$$

$$\omega \text{ (total divergence)} = \{(\text{source size})^2 + (\text{intrinsic})^2 + (\text{detector})^2\}^{1/2}$$

$$\omega_1 = h/(r-k) (k/R \sin \theta_0 - 1)$$

$$\omega_2 = \omega_D$$

$$\omega_3 = (\Delta r/d) \{ (1/R - \sin \theta_0/r) / (2/R - \sin \theta_0/r) \}$$



The source size contribution is minimized when:

$$k = R \sin \theta_0$$

i.e. when the detector is on the Rowland circle
and the sample is midway between crystal and detector.

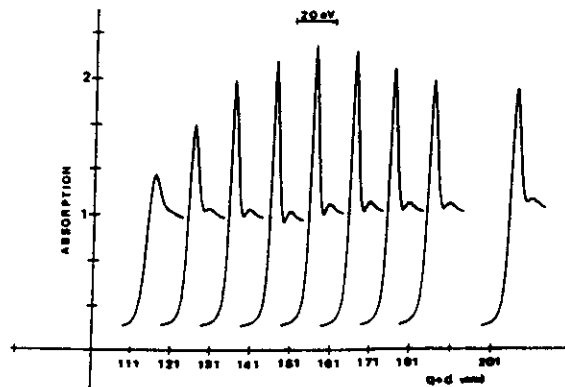


Fig. 6. The energy resolution as a function of the detector distance from the Si 311 crystal monochromator is clearly seen by the attenuation of the strong white line at the arsenic K edge of a chalcogenide sample As₂S₃.

- Cylindrical curvature of the crystal causes the presence of aberrations in the spot size:

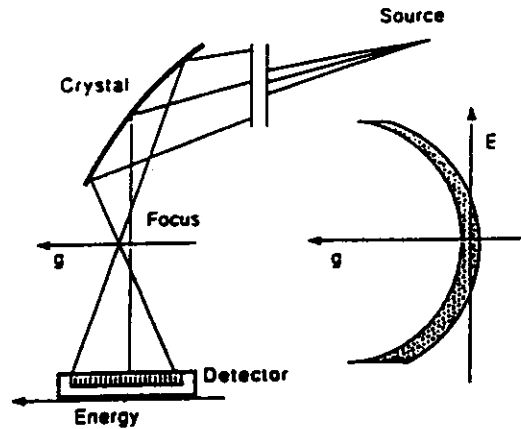


Fig. 2. The cylindrical optics produces a nonhomogeneous distribution of the rays around the focus point. This geometrical aberration, which is proportional to the square length of the crystal, is a prohibitive limitation for XAS in dispersive mode when working with very small samples because only a portion of the energy bandpass goes through them.

This can be eliminated e.g. by machining the contour of the crystal so that it will bend into an ellipse:

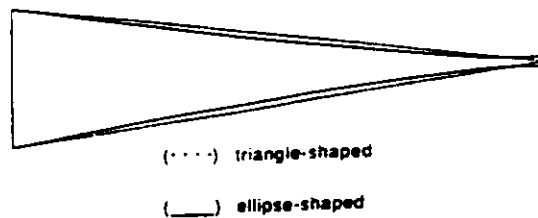


Fig. 6. (.....) Triangle-shaped crystal and (——) correction to the linear variation of the width. The crystal is shaped to provide an ideal focus from 90% of the full length.

OPTICS OF DISPERSIVE X-RAY ABSORPTION SPECTROMETERS: A STATE OF THE ART BEAMLINE: ID24 AT ESRF

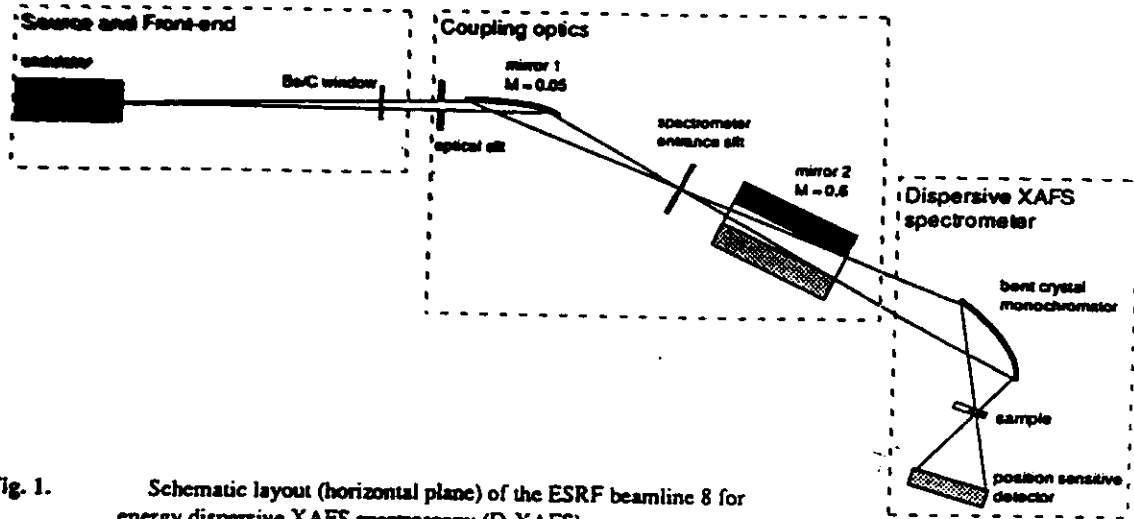


Fig. 1. Schematic layout (horizontal plane) of the ESRF beamline 8 for energy dispersive XAFS spectroscopy (D-XAFS).

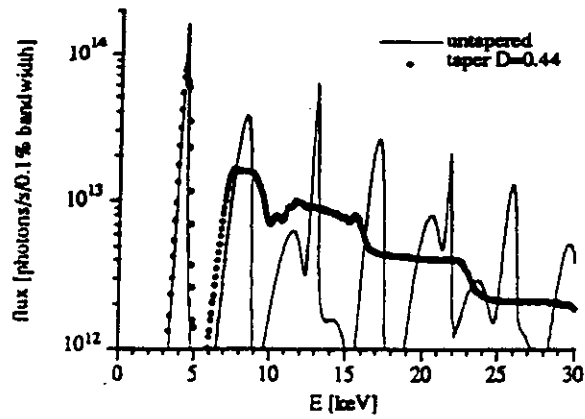
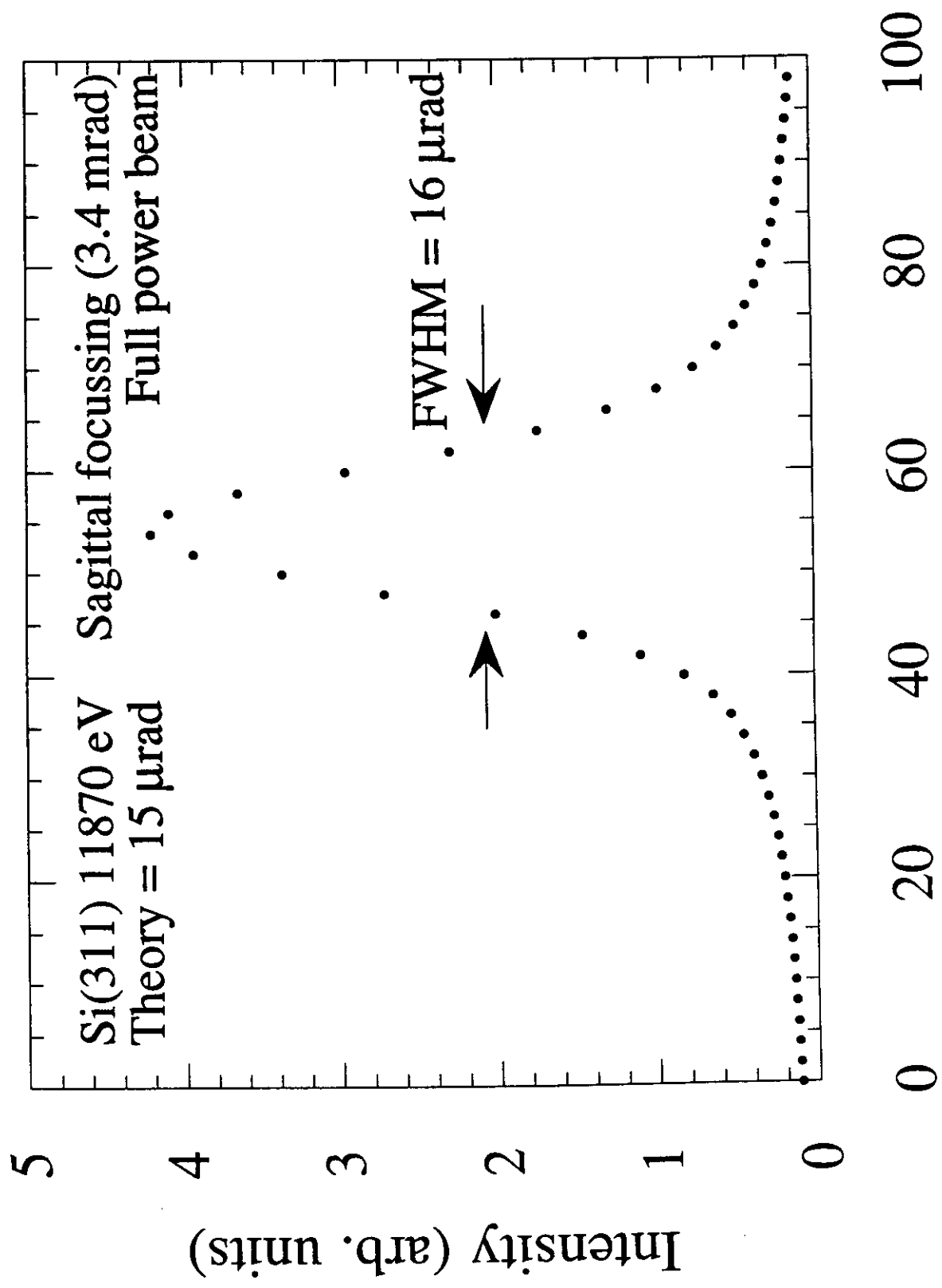


Fig. 3. Calculated flux¹⁴⁾ through a 2x2 mm² pinhole on axis 30 m from the source for the untapered and the tapered undulator (42 periods of 40 mm, K = 1.38 (at minimum gap)).

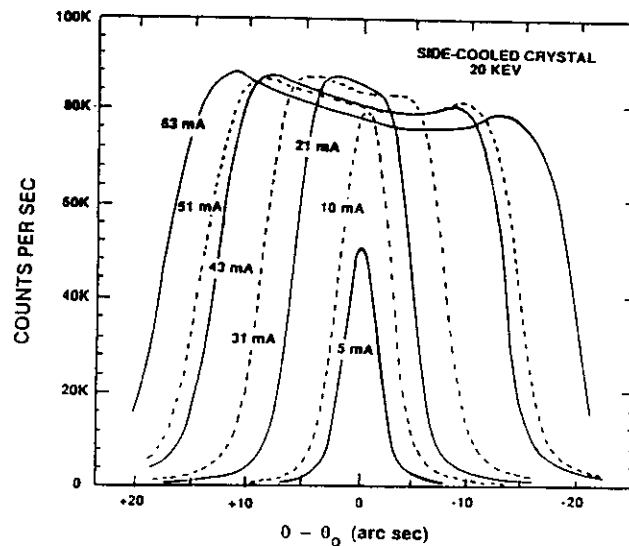
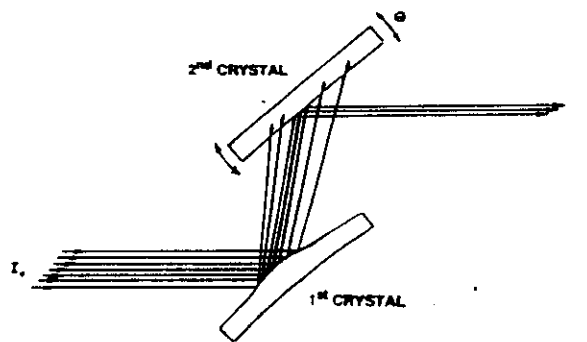
GILDA D8 - Double crystal rocking curve



HEAT LOAD

- The heat load on the first crystal of a monochromator can be very high, especially on 3rd generation machines, e.g. for ESRF:

Bending magnet: Total power ~ 200 W, Power density ~ 1 W/mm²
Undulator: Total power ~ 2 kW, Power density ~ 40 W/mm²
Wiggler: Total power ~ 10 kW, Power density ~ 20 W/mm²

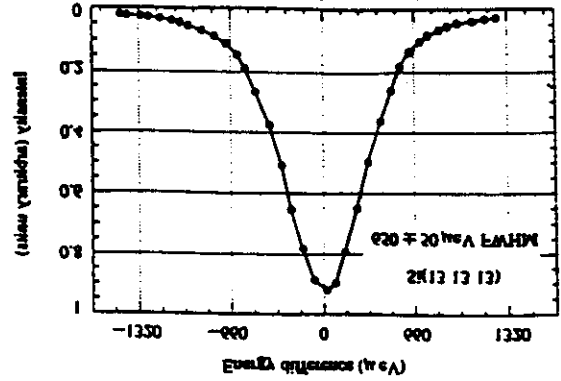


- Solutions:

⇒ Cryogenic cooling (thermal exp. of Si = 0 near LNT)

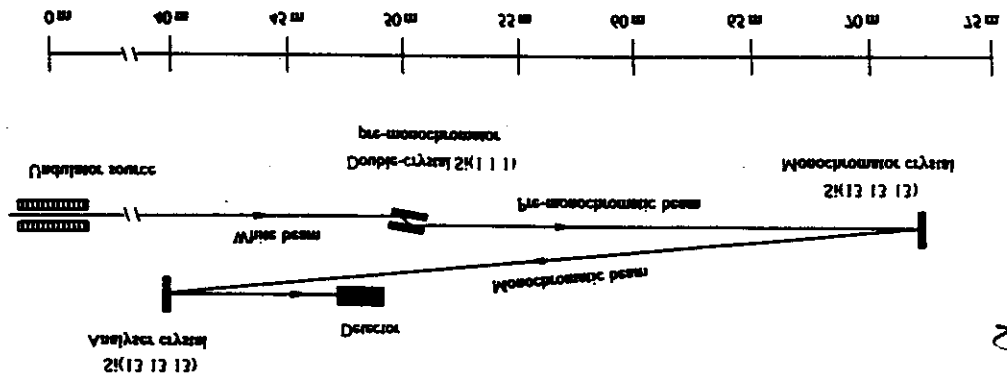
⇒ Thin crystals + water cooling

⇒ Judicious use of filters



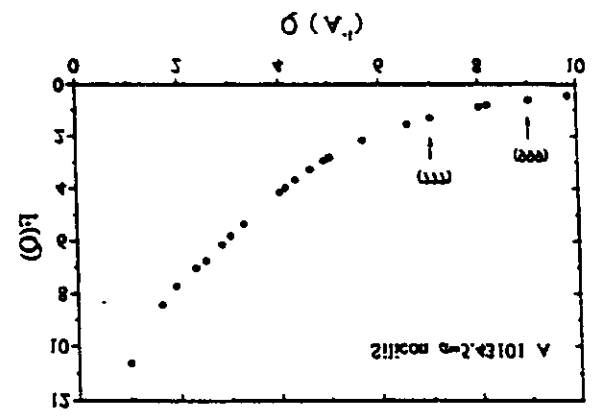
$3 \cdot 10^{-2} \text{ keV}^2$
 $\frac{E}{\Delta E} = 5 \cdot 10^{-8}$

... the error of the beam ...
 ... the resolution ... $\theta = 80^\circ$...
 ... the experimental set-up ...
 Figure 1



$\frac{y}{R} = \frac{d}{R} = \frac{1}{R}$
 ...

...
 ...



\Rightarrow very low values of $\Delta V/V$ can be reached
 \Rightarrow ωD can match the divergence of 2K source: high flux
 in nearly back-scattering geometry ($\theta_B \approx 90^\circ$), with high order reflections:

$\Delta V/V \sim q_5 FH$
 • $\omega D = 2LFH/2 \sin \theta_B \sim q_5 L \sin \theta_B FH$

- \Rightarrow Complementary to inelastic neutron scattering.
- \Rightarrow Dynamics of density fluctuations.
- Used in inelastic X-ray scattering measurements:

OPTICS FOR VERY HIGH ENERGY RESOLUTION

References

General

- T. Matsushita and Hashizume, in Handbook on Synchrotron Radiation vol 1A, edited by E.E. Koch, North Holland, Amsterdam, 1983.
- R. Caciuffo, S. Melone, F. Rustichelli, and A. Boeuf, Phys. Rep. 152, 1, (1987).

Dynamical theory

- B.E. Warren, X-Ray Diffraction, Addison Wesley, Reading MA, 1969.
- B.W. Batterman and H. Cole, Rev. Mod. Phys. 36, 681 (1964).
- R.W. James, The Optical Principles of the Diffraction of X-Rays, Bell, London, 1965.

Sagittal Focussing

- C.J. Sparks, G. Ice, S.B. Borie, J. Hastings, Nucl. Instrum. Methods 172, 237 (1980).
- J. Hrdy, Rev. Sci. Instrum. 65, 2147 (1994)
- S. Pascarelli, F. Boscherini, F. D'Acapito, J. Hrdy, C. Meneghini and S. Mobilio, J. Synchrotron Radiation 3, 147 (1996).

Dispersive XAFS

- R.P. Phizackerly, Z.U. Rek, G.B. Stephenson, S.D. Conradson, K.O. Hodgson, T. Matsushita, and H. Oyanagi, J. Appl. Cryst. 16, 220 (1983).
- H. Tolentino, E. Dartyge, A. Fontaine and G. Tourillon, J. Appl. Cryst 21, 15 (1988).
- F. D'Acapito, F. Boscherini, A. Marcelli, and S. Mobilio, Rev. Sci. Instrum. 63(1), 899 (1992).
- M. Hagelstein, A. Fontaine and J. Goulon, Jpn. J. Appl. Phys. 32, 240 (1993).

High resolution instrument for X-ray Inelastic scattering

- R. Verbeni, F. Sette, M. Krisch, U. Bergmann, B. Gorges, C. Halcoussis, K. Martel, C. Masciovecchio, J.F. Ribois, G. Ruocco and H. Sinn, J. Synch. Rad. 3, 62 (1996).

